High Voltage

Research Article

Ageing and reliability of electrical insulation: the risk of hybrid AC/DC grids

eISSN 2397-7264
Received on 18th December 2019
Revised 6th March 2020
Accepted on 1st April 2020
E-First on 8th June 2020
doi: 10.1049/hve.2019.0371
www.ietdl.org

Gian Carlo Montanari[1], Peter Morshuis[2] ✉, Paolo Seri[3], Riddhi Ghosh[3]

[1]*CAPS, Florida State University, Tallahassee, USA*
[2]*School of Electrical Engineering, Xi'an Jiaotong University, Xi'an, People's Republic of China*
[3]*University of Bologna, Bologna, Italy*
✉ *E-mail: peter.morshuis@dielectrics.nl*

Abstract: With an impetuous growth of DC links and future grids that will be often hybrid, providing AC and DC supply to nearby or the same customer, an important element is often neglected, that is, electrical insulation. There are no doubts that overhead lines will step back compared to insulated cables, for known reasons of environmental impact, right of way and reliability, especially in an urban or harsh environment. On the other hand, while AC insulation systems have been investigated and used for decades, there is no analogue experience for DC polymeric insulation, nor for insulation systems subjected to power electronics supply. This study aims at enhancing the attention on this topic, focusing on insulation ageing mechanisms and models of relevance for hybrid AC/DC assets and grids. Ageing and life models for AC, DC and power electronics supply are discussed and compared to experimental data, focusing on partial discharge and space charge. It is shown how these two phenomena affect lifetime for different AC, DC and transient operating conditions. The main drivers for insulation design and material selection are discussed, showing that insulation reliability can be achieved only if operating stresses, ageing mechanisms and life models are known and accounted for properly by insulation designers.

1 Introduction

The development of hybrid AC/DC assets in transmission and distribution links involves massive use of AC/DC, DC/AC and DC/DC converters, which depending on short circuit power, may affect the voltage waveform introducing high-frequency harmonics under AC and harmonics plus ripple under DC. A good example is the rapid development of hybrid grids in China [1], where UHVDC overhead lines bring renewable energy to the population centres in the east of China. UHVAC (800 kV and higher) lines connect this transmission system to an extensive AC distribution grid.

The impact on insulation design will be most significant in UHVDC (800 kV and higher) and HVDC (underground) cable systems. While at present the integration of HVDC cables in the power grid is still limited, in the coming decade a major leap in the installation of UHVDC and HVDC cables will be seen. In Germany, some 6000 km of HVDC cable are being installed to reinforce the existing grid and to create a power corridor that connects the wind farms in the north with the load centres in the south. For Europe, ENTSO-E and EUROPACABLE made a prognosis of the total network development required to realise the EU's commitment of a low-carbon economy by 2050 [2]. The prognosis is that some 42,600 km of HVDC land and submarine cable are needed until 2030. These, mainly polymeric-type, cables and their accessories will be operated in a hybrid AC–DC environment, leading to electrical and thermal stresses that will be different and might be higher than those considered in the design process. This may have a serious impact on insulation system reliability and life [3–6].

Choosing the proper insulation compound for such cable systems is not self-evident as is described in detail in [7]. Traditionally, HV and ultra-HV cable technologies have evolved through the refinement and upgrading of systems initially tested and proven at lower voltages. The coupling of electrical and thermal issues that will control cables of high ampacity in hybrid grids asks for an approach that can link material characteristics and cable design to anticipated grid operational conditions.

The hybrid use of cables, which could be operated either at DC or AC depending on power flow strategies, will be further promoted by the development of more reliable and versatile power conversion modules, able to provide HV and MV AC/DC/AC conversion using multi-level pulse width modulation (PWM) inverters and ultra-fast, low-loss, switches.

Such an evolving framework is tending to re-shape drastically transmission and distribution worldwide. However, while attention is paid to problems on control, switchgear and technology related to the conversion of AC lines to DC or hybrid DC–AC operation, almost no investigations are made on the reliability of an essential component of HV or MV apparatus, that is, electrical insulation [8–10].

This paper has the purpose to deal with the most important degradation mechanisms occurring in insulation under DC, AC and power electronics voltage waveforms, highlighting the effect of AC, DC and time-varying stress on life and reliability.

In Section 2, life and ageing models are discussed for constant stress and time-varying electrical stress on ageing and the relevant electro-thermal models. Section 3 eventually highlights how important ageing factors as partial discharges (PDs) and space charge are affected by a change from AC to DC power supply for an insulation system.

2 Electro-thermal stress and ageing modelling

2.1 Stresses affecting insulation systems

Typical stresses for electrical insulation in HV and MV applications are Thermal, Electrical, Ambient (Environmental) and Mechanical (TEAM) [11]. Insulation system design has the purpose to determine the maximum level of operating TEAM stresses that can ensure the design life at a chosen reliability level. The most important stresses during service of each component can be considered to simplify the design and life modelling. As an example, for HV and MV cables, thermal and electrical stresses are generally predominant (the former only for low voltage). Electrical and thermal overstress have to be taken also into account. Electrical overstress may give rise to phenomena such as accelerated global ageing, accumulation of space charge, and, locally (in defects), the inception of PDs and electrical trees.

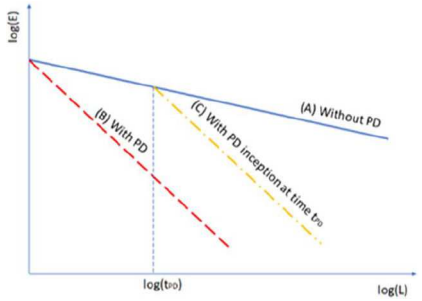

Fig. 1 *Qualitative behavior of electrical life lines with and without the occurrence of PD (straight lines on log-log coordinate system, according to (6)). A: no PD. B: PD incept during operation at time t_{PD}. C: PD incept at the beginning of load operation*

Thermal overstresses will increase the global ageing rate (e.g. oxidation rate) and raise the risk of thermal runaway in the presence of hot spots.

Focusing on electro-thermal stress, there are two fundamental considerations that a designer has to take into account. One is that permanent or transient overstresses will occur during life, the other is that factors of influence able to significantly accelerate the ageing rate, and thus shorten the life (i.e. decrease reliability) may be initiated by overstress or by local or overall ageing [12, 13].

An example that summarises both stress and factors of influence is the inception of PDs in insulation defects due to repetitive transients associated with commutation switching of power electronics in converters. While for the insulation of rotating machines fed by PWM supplies there are standards for insulation design, quality control and acceptance tests [14, 15], there is still a lack of specifications for other grid-asset components, like cables. To face the modelling problem under power electronics supply, perhaps oversimplifying but at least providing guidance, a general approach like that in the following may help. The key points, which hold for any type of supply waveform, that is, from DC to AC and power electronics supply, are:

- The ageing rate, thus life depends on the maximum stress amplitude. The larger the amplitude the shorter life, and this can be quantified by proper life models.
- The presence of factors of influence which affect the ageing rate at a given design stress amplitude is taken into account by the previous point in the list. If a factor of influence introduces an ageing mechanism that is different compared to the design stress, such as in the case of space charge or PD inception during operation which increases the electrical stress ageing rate, [16], an activation-energy term must be modified in the life model.
- Both stress and factor of influence might be time-varying, thus they 'consume' part of the life only for the time they are present during operation. This requires the use of dynamic ageing and life modelling.

2.2 General ageing model

A general definition of the ageing function, A, is [17, 18]:

$$A = F(p) = K(S)t \tag{1}$$

where p is a diagnostic property (whose time behaviour is sensitive to irreversible degradation of the insulation), S is stress, $K(S)$ is the ageing rate and t is time under stress. When p reaches a limit value, p_L, beyond which the insulation does not withstand reliably the stress(es), time becomes failure time, t_F, and the total time from the beginning of insulation operation is life, L:

$$A_L = F(p_L) = K(S)L \tag{2}$$

The ageing rate can be exploited as a function of stress knowing the ageing mechanism or, at least, a phenomenological description of the life dependence on stress (life model). As an example, for electrical stress and temperature, E and T, respectively, it holds:

$$K(E) = A'_L E^n \tag{3}$$

$$K(T) = A'_L \exp(-\Delta W/T) \tag{4}$$

where n is the voltage endurance coefficient (VEC), and ΔW the activation energy of the thermal degradation process [19, 20].

It is self-evident that the meaning of n is also that of activation energy of the electrical degradation process, even if the model (3) is purely phenomenological, while model (4) is derived from the Arrhenius thermally-activated reaction theory [20]. Equations (3) and (4) are linearised in log-log and semi-log plots, respectively, and extrapolated to design stress and life from the results of accelerated life tests. Hence, knowing the operating stress(es), the design can reach the specification goals of life and reliability for an insulation system.

Focusing on electrical stress, once the operating voltage and the design field providing the specified life and failure probability are known, the insulation thickness can be derived. Reliability is introduced in this framework through a probability distribution function which, in the case of electrical stress, is generally the Weibull distribution [21, 22]:

$$F(t_F) = 1 - \exp\left[-\left(\frac{t_F}{\alpha}\right)^{\beta}\right] \tag{5}$$

where α and β are scale and shape parameters, respectively.

2.3 Life models at constant stress

Considering stresses that do not vary (in peak value) with time, and observing that α is the failure time at probability 63.2%, a generalised probabilistic electro-thermal life model can be obtained from (5) exploiting α, as, e.g. (from (3)):

$$L = t_0\left(\frac{E}{ES_0}\right)^{-n} \cdot \frac{f_0}{f} \tag{6}$$

where f_0 is the reference frequency (e.g. 50 or 60 Hz), ES_0 is reference electric stress (generally close to the electric strength), t_0 is failure time at applied field $E = ES_0$. The quantities in the model (6) depend on temperature.

The inception of ageing-accelerating phenomena such as PD, which is the most harmful ageing factor for organic insulation under AC or power electronics supply, does not change the model, but it does change its parameters, particularly the VEC. Indeed, because ageing under PD involves a different ageing mechanism compared to that under electrical stress and no PD, the reaction rate in (3) is modified by a decrease of n (lower activation energy). An example is provided by Fig. 1, which reports qualitatively the behaviour of electrical lifelines with and without the occurrence of PD (straight lines on the log-log coordinate system, according to (6)). At constant electric stress (as that corresponding to design field), life under PD becomes dramatically shorter.

This approach is traditionally applied to design insulation systems under AC, where electric stress is generally constant as a function of operation time (apart from sporadic switching and lighting voltage transients). The challenge is to extend it to DC and power electronics waveforms, as well as to time-variable electric stress.

An observation which is approximate, but able to strongly simplify the problem, is that it is commonly accepted that the major driver for electrical ageing is peak (or peak-to-peak) voltage, see e.g. IEC 60034-18-42 [15].

This would allow to use (6) also for power electronics waveforms, in the absence and presence of PD, considering the modulation frequency f, and the peak value of the maximum electric field, which is determined by two factors [14]:

- transient peak voltage at each switching (associated with wave reflection in the cable connection inverter and load, besides switch rise time), see Fig. 2;
- uneven voltage potential distribution when the load is a rotating machine winding (due to the inductive component of the load impedance).

It is noteworthy that, according to model (6) and contrarily to what is assumed in IEC standards [14, 15], accelerated ageing occurs, compared to an insulation system designed at power supply frequency $f_0 = 50$ or 60 Hz, the more the modulation frequency exceeds the power supply frequency, thus also in the absence of PD. Fig. 3 shows experimental life lines obtained for insulated wires aged at 50 Hz (f_0) and 10 kHz (f) with and without PD (the former tests were performed in air, the latter in oil, to avoid PD inception [23–25]). The values of VEC (6) decrease significantly under PD, while they do not change as much with frequency. The increase of frequency, however, reduces life, according to model (6), by about 200 times (f/f_0) in the absence of PD, while the effect of life reduction due to frequency is more dramatic in the presence of PD, owing to the large influence of frequency on the PD-related damage growth process. Other factors contribute to reduce life under power electronics compared to AC, particularly the switch rise time and the number of inverter levels, [25], but this is not considered here.

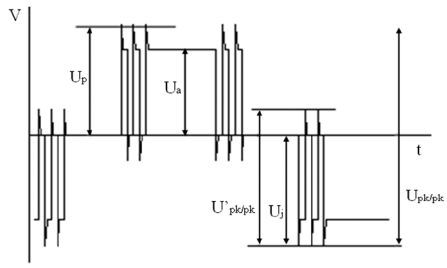

Fig. 2 *Example of a voltage waveform at the terminals of a two-level voltage-converter fed load, where the commutation peak voltage is highlighted. U_a = inverter dc-bus voltage, U_P = peak voltage at the load terminals, $U_{pk/pk}$ = peak-to-peak voltage at the fundamental frequency, $U'_{pk/pk}$ = peak-to-peak voltage at the impulse repetition frequency. U_j = jump voltage*

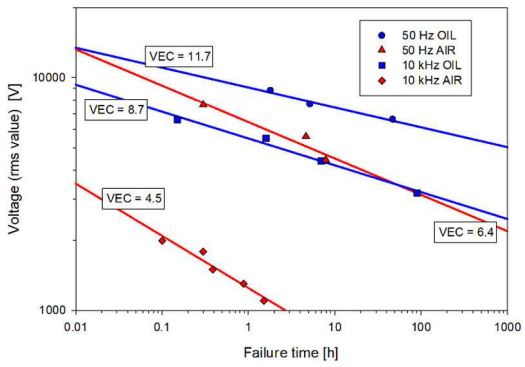

Fig. 3 *Experimental life lines obtained for insulated wires aged at 50 Hz (f_0) and 10 kHz (f) with PD (tests in air) and without PD (tests in oil). The values of VEC from (6) are reported*

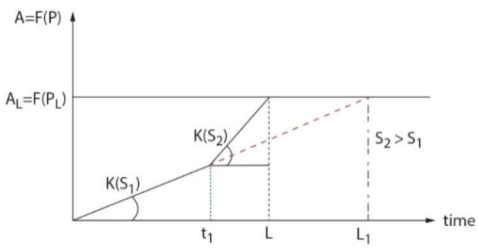

Fig. 4 *Ageing function, (1), (2), as a function of time, for two different stress magnitudes, S1>S2*

Equation (6), upon removing the frequency term, can be used also under DC, again referring to the maximum electric field. In case of non-uniform electric field geometries, as for cables, the field profile under DC can be significantly different from AC, thus the maximum field has to be properly calculated depending on the applied voltage, insulating material characteristics and operating temperature.

2.4 Time-varying electrical stress and ageing modelling

For transmission and distribution networks containing DC and AC apparatus, in the presence of power converters and inverters it can no longer be expected that the magnitude of the electric stress is constant in time, apart from sporadic switching and lighting transients, as in conventional AC networks. Switching harmonics, resonances, repetitive overvoltage impulses, voltage sags and drops, repetitive transients as those involving renewables interconnection, DC ripple, DC apparatus energisation, DC cable voltage polarity inversion and so on have to be taken into account by the electrical ageing models described in the previous section.

Considering (1), (2), if the stresses change in magnitude and/or the activation energy of the ageing process varies (e.g. due to PD inception and extinction), the ageing rate will vary dynamically, as a function of time. The ageing equation can be thus rewritten, through a convolution integral, as [12]:

$$F(P) = K(S(\tau)) * t \tag{7}$$

As an example, Fig. 4 shows the behaviour of the ageing function when at time t_1 the stress amplitude increases. Life, L, becomes shorter compared to life L_1 pertinent to (design) stress S_1.

A simplified approach to model (7) is based on the superposition effect (Miner law), that is [26]:

$$\sum \frac{t_i}{L(S_i)} = 1 \tag{8}$$

where t_i is time under stress S_i and $L(S_i)$ the relevant life which can be expressed by (6). A broader and more comprehensive approach was presented in [12, 27–29] leading to a generalised probabilistic model that can account for practically any type of time-varying voltage waveform. Accordingly, the insulation reliability $R = 1 - F$ can be determined for overvoltage transients of known mean repetition rate and voltage magnitude probability density:

$$R(t) = \mathrm{e}^{-\left[t_F \cdot \left(\frac{1}{t_{\mathrm{ac}}}\left(\frac{E_{\mathrm{ac}}}{E_{S0\mathrm{ac}}}\right)^{n_{\mathrm{ac}}} + \frac{f}{f_0}\int_0^{E_{\mathrm{p},99\%}} \frac{1}{t_{\mathrm{p}}}\left(\frac{E_{\mathrm{p}}}{E_{S0\mathrm{p}}}\right)^{n_{\mathrm{p}}} f(E_{\mathrm{p}})\mathrm{d}E_{\mathrm{p}}\right)\right]^{\beta}} \tag{9}$$

where $E_{S0\mathrm{ac}}$ and $E_{S0\mathrm{p}}$ are the electric strength measured under AC and transient voltage impulses, respectively. E_{ac} and E_{p} are the electric stress under AC and overvoltage transient impulses. n_{ac} and n_{p} are the VEC (relevant to AC and impulsive stresses (from (8)). t_{ac} and t_{p} are the times of application of ac and voltage impulse stresses. f is the mean overvoltage occurrence frequency and f_0 is the AC voltage frequency. $f(V_{\mathrm{P}})$ is the probability density function of the random variable E_{P}, so that $f(E_{\mathrm{P}})\mathrm{d}E_{\mathrm{P}}$ is the frequency of occurrence of a given voltage impulse with an electric field amplitude in the range $[E_{\mathrm{p}}, E_{\mathrm{p}} + \mathrm{d}E_{\mathrm{p}}]$. β is the shape parameter of the Weibull distribution of failure times, (5).

If, just for simplification, reference is made to (8) for a two-level stress variation which occurs for total times t_1 and t_2 during operation, the resulting life, $L = t_1 + t_2$, can be obtained:

$$\delta\frac{t_2}{L_1} + \frac{t_2}{L_2} = 1 \tag{10}$$

with $\delta = t_1/t_2$. L_1 and L_2 can be obtained through the inverse-power model (6) (without the frequency ratio in case of DC stress).

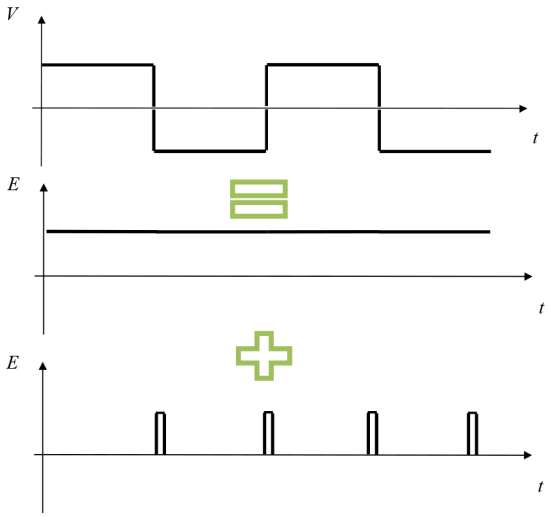

Fig. 5 *Time evolution of the applied voltage in a HVDC transmission cable with polarity reversal (above) and decomposition for ageing rate calculation based on superposition effect (below)*

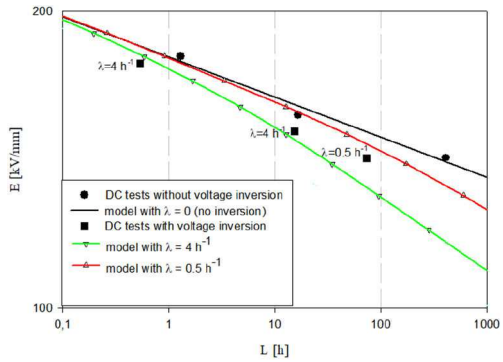

Fig. 6 *Experimental results of life tests performed on polymeric cable models, at failure probability 63.2%, with and without voltage polarity inversion (at inversion rate 0.5 and 4 h^{-1}). The life lines fitting to (6), for life without polarity inversion, and (14), for life with polarity inversion, are reported*

To support the validity of a superposition effect ageing model, let us consider a practical case of a DC cable subjected to repeated voltage polarity inversions. During supply voltage variation, as it will be shown in the next section, PD can incept, thus the ageing rate will increase significantly for the duration of the electric field transient (which can last even thousands of minutes). Fig. 5 displays the supply voltage waveform and the resulting superposition effect, for the ageing rate calculation, under the assumptions that [29]:

- a positive steady applied electric field, of magnitude E, is equivalent, from the viewpoint of material ageing, to a negative electric field of the same intensity (as mentioned, ageing rate is governed by the stress peak value);
- all the processes related to voltage reversal are confined within the time (relatively short, compared to life) starting with and ending immediately after the inversion.

Based on (1), (2), and Fig. 4, it can be written:

$$\frac{1}{L(E,\lambda)} = \frac{1}{L(E)} + \frac{1}{L(\lambda_E)} \tag{11}$$

where $L(E,\lambda)$ is insulation life at a field E with polarity reversal at the frequency λ, $L(E)$ is life at a constant field E, $L(\lambda_E)$ is life due only to pulses of amplitude E and frequency λ, see Fig. 5. If $N(E,\lambda)$ is the total number of pulses to failure in the former case and N_E that in the latter, since $N(E,\lambda) = \lambda\, L(E,\lambda)$ and $N_E = \lambda\, L(\lambda_E)$, it follows that:

$$\frac{L(E,\lambda)}{L(\lambda_E)} = \frac{N(E,\lambda)}{N_E} = \frac{\lambda L(E,\lambda)}{N_E} \tag{12}$$

then:

$$\frac{L(E,\lambda)}{L(E)} + \frac{\lambda L(E,\lambda)}{N_E} = 1 \tag{13}$$

which has the same form as the superposition effect model (8). The life under maximum electrical stress E and voltage polarity inversion at rate λ, $L(E, \lambda)$, can be then derived as:

$$L(E,\lambda) = \frac{1}{(1/L(E)) + \dfrac{\lambda}{N_E}} \tag{14}$$

Fig. 6 shows experimental results of life tests performed on polymeric cable models with and without voltage polarity inversion (at inversion rate 0.5 and 4 h^{-1}), fitting to the inverse-power model, (6), for life without polarity inversion, and (14) for life with polarity inversion. It is noteworthy that the fit to model (6) is quite good, for points without voltage inversion, but also that the life points with $\lambda = 0.5$ and 4 h^{-1} are close to the theoretical lines drawn by means of (14) for such frequencies. There is, however, an implicit assumption in the model, that is, N_E inversions of amplitude E are needed to breakdown insulation irrespectively of the inversion frequency, λ.

It is noteworthy that while accelerated life modelling needs to be supported by sufficient experimental data, its procurement requires generally long and expensive testing. The merit of a global approach, as presented here, is also in driving testing procedures and providing qualitative and quantitative assessment of the potential effect of stresses on ageing processes and insulation design.

3 Factors of influence accelerating the ageing process under DC and AC: field distribution, PDs and space charge

3.1 Electric field distribution

The distribution of the electric field under steady-state DC and AC voltage is driven by conductivity and permittivity, respectively [30–33]. Since the dependence on temperature of conductivity, which is described by an Arrhenius-type law holding a temperature coefficient, α, [20, 31], is strong, while that of the permittivity is negligible, the electric field profile in an insulation system can be significantly different, especially for systems where the field distribution is not uniform, such as cables. The cable loading, which gives rise to a temperature gradient in the insulation, can cause a field profile in DC cable insulation which is opposite to that under AC voltage, with a maximum field at the outer semicon rather than at the inner one [30]. As an example, Fig. 7 reports the field profiles in a 50 kV polymeric cable supplied under AC or DC steady-state, at the same maximum voltage and insulation thickness, with a temperature gradient of 10°C (when under full load). Already with a quite small temperature gradient, under steady-state DC the electric field profile is inverted compared to AC, and also the maximum electric field value becomes higher. This may reflect a shorter life, as indicated by (6) and Fig. 1.

Most importantly, the modification of the electric field profile in the insulation and its defects (cavities) under DC steady-state can translate into a different capability, compared to AC, to activate PD in insulation cavities. Indeed, if defects near to the inner semicon might generate PD under AC, because of the higher field, in DC steady-state (and under load) PD will be activated more likely by defects closer to the outer semicon [34–38].

The physical mechanism of PD under DC voltage is approximately the same as under AC, being driven by field magnitude, electron injection probability and gas-ionisation features [16, 34, 39]. The phenomenology of PD under DC and AC is however significantly different, particularly in terms of repetition

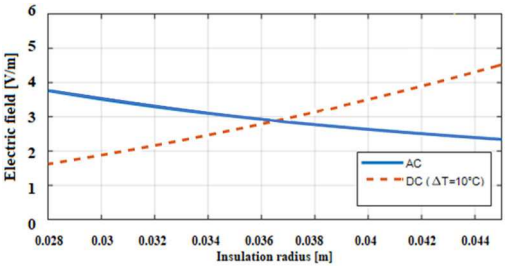

Fig. 7 *Field profile in a polymeric cable under AC or DC steady-state, for the same maximum voltage and insulation thickness. 50 kV polymeric cable, 17 mm insulation thickness and a temperature gradient, ΔT, under DC of 10°C. Relative permittivity 2.3, $\gamma_0 = 1.710^{-19}$ Sm^{-1} (conductivity at 0°C), $\alpha = 0.16°C^{-1}$(temperature coefficient of conductivity)*

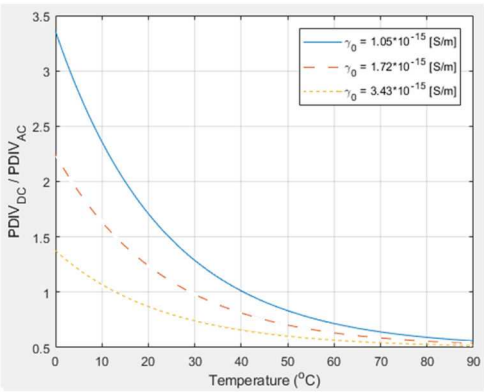

Fig. 8 *Ratio of $PDIV_{DC}$ to $PDIV_{AC}$ as a function of temperature (model (15)) and conductivity at 0°C, γ_0, for polymeric specimens of mean thickness $h_b = 1.22$ mm, containing and embedded cavity of height $h_c = 0.41$ mm. Relative permittivity of the polymeric material = 2.3. After [35]*

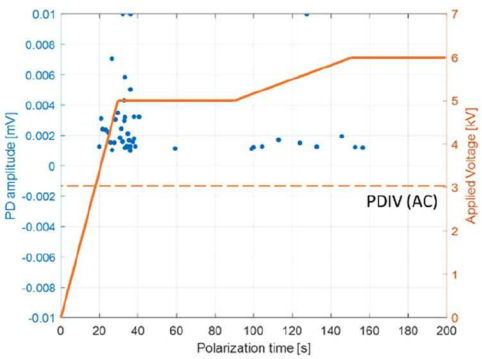

Fig. 9 *PD events during energisation of a DC insulation system (test object made by polymeric films with a cavity having height $h_c = 0.1$ mm). The voltage is applied in two steps: from 0 to 5 kV in 30 s, then steady at 5 kV for 1 min and from 5 to 6 kV in 1 min. The PDIVAC measured at 50 Hz is indicated*

rate and magnitude [3, 36, 40]. This impacts significantly on the ageing rate and life and therefore the following discussion will mostly focus on those parameters, i.e. PD inception voltage (PDIV), PD repetition rate and magnitude.

Field intensity variation and distribution can also affect space charge, which has also to be investigated as one of the potential harmful accelerated-ageing mechanisms under DC voltage supply.

As a note, such findings highlight clearly that testing DC insulation under AC can provide useful information about the presence of defects, but not about the operating behaviour and ageing under steady-state DC electrical stress. Defects that in practice would lead to PD under DC may however remain undetected in AC tests.

3.2 PDs in DC steady-state and transient voltage conditions

As a striking consequence of the difference between AC and DC field regimes, the PDIV, varies dramatically from AC to DC. Considering, for example, a flat cavity of height h_c, in a uniform-field geometry insulation system, the ratio between DC and AC PDIV is [35]:

$$\frac{\mathrm{PDIV_{DC}}}{\mathrm{PDIV_{AC}}} = \frac{\varepsilon_b}{\gamma_b} \cdot \frac{\gamma_b h_c + \gamma_c(h_b)}{\varepsilon_b h_c + \varepsilon_c(h_b)} \tag{15}$$

with ε_b, γ_b and ε_c, γ_c the permittivity and conductivity of insulation and cavity (generally filled with air), respectively, and $h_b = d - h_c$ where d is the insulation thickness [35].

Fig. 8 displays the ratio of $\mathrm{PDIV_{DC}}$ to $\mathrm{PDIV_{AC}}$, from (15), as a function of temperature and conductivity, for polymeric specimens of mean thickness $h_b = 1.22$ mm, containing an embedded cavity of height $h_c = 0.41$ mm. As can be seen, $\mathrm{PDIV_{DC}}$ is generally higher than $\mathrm{PDIV_{AC}}$ at room temperature, due to the low conductivity of the insulation. However, $\mathrm{PDIV_{DC}}$ can become lower than $\mathrm{PDIV_{AC}}$ when the conductivity increases with temperature and it becomes larger than that of the cavity gas, i.e. under full load (for this example $\mathrm{PDIV_{DC}}/\mathrm{PDIV_{AC}}$ ranges between 3.4 and 0.5 increasing temperature from 20 to 90°C). Hence, dielectrics with as low conductivity as possible would be best candidates for DC insulation, thus making it possible for a DC insulation system to work, in steady-state, below $\mathrm{PDIV_{DC}}$, while under AC the conductivity becomes an issue only due to dielectric losses (thus mostly under EHVAC).

This picture, however, is complicated by energisation and, if present, voltage polarity transients (modelled in the previous section) which will occur during operation of a DC insulation system. During time variation of supply voltage, the electric field inside the insulation will be driven by the permittivity, as in AC, not by the conductivity, as in DC steady-state. Therefore, PD can incept according to $\mathrm{PDIV_{AC}}$, thus below $\mathrm{PDIV_{DC}}$ even if the insulation system was designed to operate below $\mathrm{PDIV_{DC}}$ in steady-state. This is the physical background of the case summarised in Figs. 5 and 6 and modelled through (14). It is noteworthy that the time constant for the electric field to reach DC steady-state is given by [31–33, 41, 42]:

$$\tau \propto \frac{\varepsilon_{\mathrm{eq}}}{\gamma_T} \tag{16}$$

where γ_T is the conductivity and $\varepsilon_{\mathrm{eq}}$ the equivalent permittivity as derived, e.g. from the time constant obtained from polarisation current measurements performed on the insulating material used for the apparatus, at the chosen steady-state DC field and temperature, [41, 42]. Typical values of conductivity and permittivity for a HV or MV polymeric insulation, at operating stresses, provide estimates of transient times of hundred minutes. Fig. 9 shows PD events during energisation of a DC insulation system, for a test object made by polymeric films with a cavity having height $h_c = 0.1$ mm. As can be seen, PD incept at the time at which the voltage exceeds the $\mathrm{PDIV_{AC}}$, thus PD are expected to occur at each energisation (or voltage polarity inversion). PD then display lower and lower repetition rate as time tends to τ. Hence, the more energisation and voltage polarity inversion transients during operation, the larger the risk of life or reliability reduction for a DC insulation system. To bring down this contribution to insulation accelerated ageing, considering that the permittivity of polymeric materials used for MV and HV electrical apparatus varies in a very narrow range, the parameter which can be maximised is the conductivity. However, this goes in the opposite direction of what is speculated above about increasing the $\mathrm{PDIV_{DC}}$ in steady-state. Therefore, compromises are needed in insulation system design and material choice to reach the best performance, but they are based on a careful survey of operating conditions, material and technology improvement and optimisation, and on dedicated modelling as that introduced in this paper.

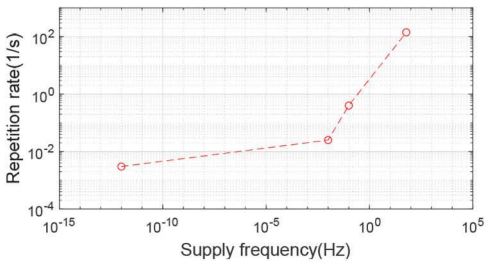

Fig. 10 *Experimental repetition rate of PD for polymeric specimens with internal cavity, as a function of frequency (from DC to AC power supply). Data measured at PDIV*

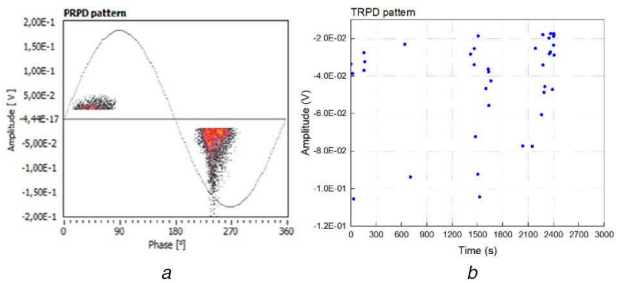

Fig. 11 *PRPD and TRPD patterns from PD measurements performed under AC 50 Hz and DC (negative voltage polarity) on a MV cable with an artificial surface defect at one termination*

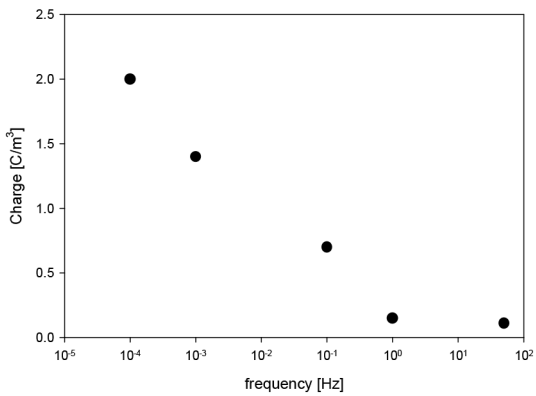

Fig. 12 *Dependence of space charge density on supply-voltage frequency. Sinusoidal voltage, poling field 55 kV/mm. Polymeric press-molded specimen. After [45]*

Regarding PD magnitude, although PDs in a cavity under DC voltage supply occur at different inception voltage, the inception field is approximately the same as under AC [34, 35]. The PD amplitude is not far from that found at AC, depending on the material characteristics, that is, on the stochastic delay time of the initiating electron [16, 35, 36]. However, the most significant difference is in the PD repetition rate, which for DC is one to three orders of magnitude smaller than for AC. Figs. 10 and 11 show the experimental results of PD measurements in the range from DC to AC power frequency voltage. Fig. 10 highlights the large increase of repetition rate as a function of frequency, from DC to AC. Fig. 11 displays the phase-resolved and time-resolved PD patterns (PRPD and TRPD, respectively) for a defect providing surface PD at termination of an MV polymeric cable under AC 50 Hz and DC (negative voltage polarity) [38]. Referring to Fig. 11, besides the clear difference in repetition rate, it must be underlined how all the experience accumulated in pattern interpretation under AC power supply, which is fundamental for condition maintenance [39, 43, 44], gets lost in DC, because of the lack of phase correlation with the voltage waveform (the same holds for power electronics waveforms [25]). This complicates, in particular, noise identification and rejection under DC, which is certainly one of the major reasons why PD measurements under DC are very seldom performed in DC insulation systems (and, e.g. commissioning tests are still carried out under AC for both AC and DC cables).

As a consequence of the very low repetition rate, even if the PD-pulse amplitude can be larger than under AC (but only in the high-amplitude part of the amplitude distribution [35]), the cumulated disruption rate of insulating-material bonds, i.e. the mechanism bringing the insulation to failure due to PD, is much smaller than under AC, thus resulting in a lower damage rate from PD under DC. This would translate into a higher VEC, (6), for the same material (but still smaller than that obtained from life lines without PD). This speculation has not been proved yet unambiguously (further experimental work is needed), but it seems likely.

3.3 Space charge

There is, however, another accelerated ageing factor which takes place under DC and it is absent under AC, that is, the accumulation of space charges in insulation. Fig. 12 shows space charge magnitude as a function of supply-voltage frequency in a typical polymer used for AC and DC insulation, that is, cross-linked polyethylene, XLPE. As can be seen, the space charge density in the tested insulating material decreases rapidly, to values near to zero, increasing frequency above DC [13, 45]. Such phenomenon, theorised already in the 1950s as affecting polymer conduction (the space charge limited conduction, SCLC, mechanism, [46], stems from it), was measured directly in the 1980s [47]. Its effect on ageing can be predicted roughly in terms of increase of maximum field inside insulation due to space charge that can modify the Laplace field (geometric) to a Poisson distribution. The extent of this cannot be predicted if not measuring space charge accumulation at the electric fields and temperatures involved in insulation design and operation [13]. Fig. 13 shows a striking example of electric field magnification in an EVA polymer (loaded by clay nanofillers) due to space charge accumulation. While the geometric (Laplace) field is 60 kV/mm, the maximum (Poisson) field reaches 200 kV/mm due to space charge accumulation. This can cause insulation breakdown under DC voltage in minutes or even seconds rather than the tens of years expected from design specifications, as highlighted by Fig. 14.

Eventually, Fig. 14 reports a summary of the above concepts relevant to PD and space charge, showing typical life lines (according to (6)) for an insulating polymer at operating temperature, with slope affected by PD. Values of initial electric strength, VEC and design life are $ES_0 = 250$ kV/mm, $n = 10$ and $L_D = 30$ years at the design field of 30 kV/mm. The presence of steady PD decreases n to 6, thus causing significant life loss compared to design life. A permanent increment of the electric field of 20% due to e.g. space charge (or e.g. DC ripple) can reduce the life by about 6 times, which becomes almost 4 orders of magnitude in the presence of PD, when they occur since the beginning of the operation, i.e. at time zero. An increase of maximum field due to space charge as that of Fig. 13 brings the field near to the electric strength, thus life to seconds [44].

4 Conclusions

Because the power grid will become more and more of a hybrid nature, extensive work has to be done on the effect of non-AC voltages on the insulation system. Ageing and failure of electrical insulation cannot be a second-level issue in a DC or hybrid grid, because it may impact deeply on grid reliability, especially on the long term. There is not enough experience on long term behaviour of electrical insulation nor on its condition monitoring under DC, power electronics, and, in general, non-sinusoidal voltage supply. The knowledge of the ageing drivers, from stresses to factors of influence (particularly of fast-accelerating ageing factors as PDs and space charge), as well as of the real operating conditions of grid apparatus during life is fundamental for the use of the ageing models dealt with in this paper and, therefore, to design insulation systems with specified reliability and life.

As a matter of fact, an important point to be recalled when dealing with hybrid systems, at HV or MV level, is that materials used for AC electrical insulation may not work for DC supply, and vice versa. The latter case, considering DC steady-state and

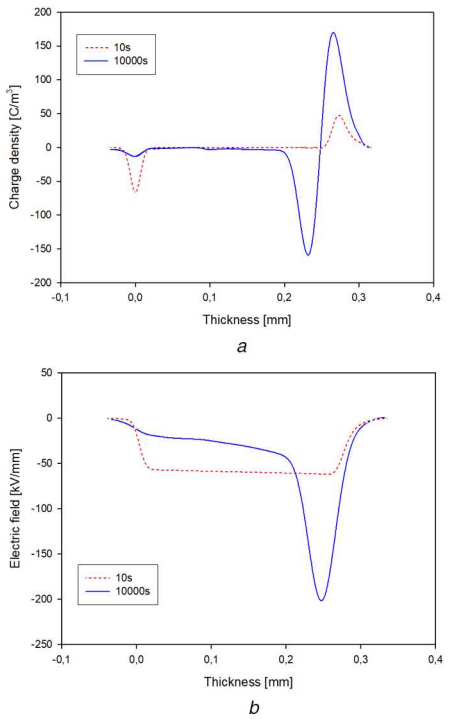

Fig. 13 *Space charge (a) and electric field profile (b) measured as a function of poling time on a nanostructured ethylene-vinylacetate (EVA) specimen at poling (Laplacian) field of − 60 kV/mm (the x-axis reports the insulation thickness). The maximum field (Poissonian) is about − 200 kV/mm at the end of poling time. Nanofiller is a clay (montmorillonite) at 5% wt density. After [13]*

(a) Space charge, ***(b)*** Electric field profile

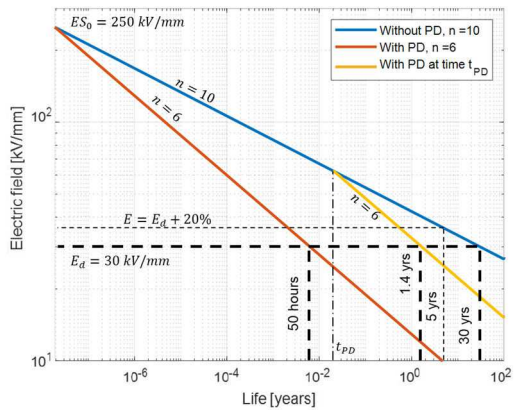

Fig. 14 *Example of life lines (according to the inverse-power law (6)) for a typical electrical polymeric insulation used in MV or HV, at operating temperature, with VEC n = 10 and life of 30 years at the design field of 30 kV/mm. Inception of PD decreases n to 6, thus causing significant life loss compared to design life whether PD incept at the beginning of operation or at time t_{PD}. A permanent increase of the electric field of 20% due to space charge can reduce the life by about 6 times*

voltage-variation transients, is a challenge for designers involving both DC and AC-like operating conditions. Hence, an electrical apparatus designed to operate in AC may not be suitable for DC, providing shorter life and reliability than specified. Since condition monitoring devices are not available yet for DC operation, this means that insulation design for DC apparatus must be conservative and well aware of working conditions. Operation in hybrid grids may require further levels of cautiousness and knowledge of ageing factors and models, as those introduced here, as well as, likely, improved insulating materials (nanostructuration may help, perhaps).

5 References

[1] Fairley, P.: 'China's ambitious plan to build the world's biggest supergrid', IEEE Spectrum, 21 February 2019, https://spectrum.ieee.org/energy/the-smarter-grid/chinas-ambitious-plan-to-build-the-worlds-biggest-supergrid, accessed 9 December 2019

[2] ENTSO-E, Europacable.: 'Recommendations to improve HVDC cable systems reliability', European Network of Transmission System Operators for Electricity, 13 June 2019, https://docstore.entsoe.eu/Documents/Publications/Position%20papers%20and%20reports/Joint%20paper%20HVDC%20Cable%20Reliability%20ENTSO-E%20Europacable.pdf, accessed 12 February 2020

[3] IEEE Recommended Practice and Requirements for Harmonic Control in Electric Power Systems, IEEE, 2014, p. 519

[4] Montanari, G.C., Cacciari, M., Cavallini, A.: 'Stochastic evaluation of harmonics at network buses', *IEEE Trans. Power Deliv.*, 1995, **10**, (3), pp. 1606–1613

[5] Montanari, G.C., Fabiani, D.: 'The effect of nonsinusoidal voltage on intrinsic ageing of cable and capacitor insulating materials', *IEEE Trans. Dielectr. Electr. Insul.*, 1999, **6**, (6), pp. 798–802

[6] Cavallini, A., Mazzanti, G., Montanari, G. C., *et al.*: 'The effect of power system harmonics on cable endurance and reliability'. Proc. 35th IEEE IAS, Rome, Italy, October 2000, pp. 3172–3179

[7] Montanari, G.C., Morshuis, P.H.F., Zhou, M., *et al.*: 'Criteria influencing the selection and design of HV and UHV DC cables in new network applications', *High Voltage*, 2018, **3**, (2), pp. 90–95

[8] de Donker, R.W.: 'Power electronic technologies for flexible DC distribution grids'. IEEE Int. Power Electr. Conf., Hiroshima, Japan, May 2014, pp. 736–743

[9] Olenmark, A., Sloth, J., Johnsson, A., *et al.*: 'Control development and modeling for flexible DC grids in Modelica'. 11th Int. Modelica Conf., Versailles, France, September 2015, pp. 823–829

[10] Montanari, G.C.: 'The potential impact of flexible DC transmission and distribution on insulated cables: accelerated ageing and premature failure'. 11th IEEE PES Asia-Pacific Power Energy Eng. Conf. APEEC, Macao, China, December 2019, pp. 1–4

[11] Evaluation and qualification of electrical insulation systems, IEC 60505, 4th ed., 2011

[12] Montanari, G.C., Seri, P., Morshuis, P., *et al.*: 'An approach to insulation condition monitoring and life assessment in emerging electrical environments', *IEEE Trans. Power Deliv.*, 2019, **34**, (4), pp. 1357–1364

[13] Montanari, G.C.: 'Bringing an insulation to failure: the role of space charge', *IEEE Trans. Dielectr. Electr. Insul.*, 2011, **18**, (2), pp. 339–364

[14] Rotating electrical machines – Part 18-41: 'Partial discharge free electrical insulation systems (Type I) used in rotating electrical machines fed from voltage converters – Qualification and quality control tests, IEC 60034-18-41', 2014

[15] Rotating electrical machines – Part 18-42: 'Qualification and acceptance tests for partial discharge resistant electrical insulation systems (Type II) used in rotating electrical machines fed from voltage converters, IEC 60034-18-42', 2016

[16] Montanari, G.C.: 'A contribution to unravel the mysteries of electrical aging under DC electrical stress: where we are and where we need to go'. IEEE ICD, Budapest, Hungary, July 2018, pp. 1–11

[17] Montanari, G.C.: 'Notes on theoretical and practical aspects of polymeric insulation ageing', *IEEE Electr. Insul. Mag.*, 2013, **29**, (4), pp. 30–40

[18] Montanari, G.C., Simoni, L.: 'Ageing phenomenology and modeling', *IEEE Trans. Dielectr. Electr. Insul.*, 1993, **28**, (5), pp. 755–776

[19] Guide for the determination of thermal endurance properties of electrical insulating materials. Parts 1-7, IEC 60216, 2013

[20] Dakin, T.W.: 'Electrical insulation deterioration treated as a chemical rate phenomenon', *Trans. Am. Inst. Electr. Eng.*, 1948, **67**, (1), pp. 113–122

[21] Montanari, G.C., Cacciari, M.: 'A probabilistic insulation life model for combined thermal-electrical stresses', *IEEE Trans. Electr. Insul.*, 1985, **20**, (3), pp. 519–522

[22] Electrical Insulating Materials – A.C. Voltage Endurance Evaluation, IEC 61251, 2014

[23] Fabiani, D., Montanari, G. C., Contin, A.: 'Ageing acceleration of insulating materials for electrical machine windings supplied by PWM in the presence and in the absence of partial discharges'. IEEE 7th Int. Conf. Solid Dielectrics, Eindhoven, The Netherlands, June 2001, pp. 283–286

[24] Montanari, G.C.: 'Power electronics and electrical apparatus: a threat?'. NORD-IS 07, Lingby, Denmark, June 2007, pp. 1–9

[25] Montanari, G.C., Seri, P.: 'The effect of inverter characteristics on partial discharge and life behaviour of wire insulation', *IEEE Electr. Insul. Mag.*, 2018, **34**, (32), pp. 32–39

[26] Miner, M.A.: 'Cumulative damage in fatigue', *J. Appl. Mech.*, 1945, **12**, pp. 159–164

[27] Montanari, G.C., Fabiani, D., Ciani, F.: 'Partial discharge and ageing of AC cable systems under repetitive voltage transient supply'. IEEE Electr. Insul. Conf., Montreal, Canada, 2016, pp. 379–382

[28] Ragaini, E., Viaro, F., Mastromauro, C., *et al.*: 'Reduction of capacitor ageing by the use of transient-free diode-based synchronous switch'. IEEE Intern. Conf. Environ. Electr. Engg., Milan, Italy, May 2017, pp. 1–6

[29] Cavallini, A., Fabiani, D., Mazzanti, G., *et al.*: 'Life estimation of DC insulation systems in the presence of voltage-polarity inversions'. IEEE Intern. Symp. Electr. Insul., Anaheim, USA, April 2000, pp. 473–476

[30] Buller, F.H.: 'Calculation of electrical stress in DC cable insulation', *IEEE Trans. Power Appl. Syst.*, 1967, **86**, (10), pp. 1169–1178

[31] Kreuger, F.H.: '*Industrial high DC voltage*' (Delft University Press, Delft, the Netherlands, 1995)

[32] Jeroense, M.J.P., Morshuis, P.H.F.: 'Electric fields in HVDC paper-insulated cables', *IEEE Trans. Dielectr. Electr. Insul.*, 1998, **5**, (2), pp. 225–236
[33] Mazzanti, G., Marzinotto, M.: '*Extruded cables for high-voltage direct-current transmission: advances in research and development*' (John Wiley & Sons, Hoboken, NJ, USA, 2013)
[34] Niemeyer, L.: 'A generalized approach to partial discharge modelling', *IEEE Trans. Dielectr. Electr. Insul.*, 1995, **2**, (4), pp. 510–527
[35] Montanari, G. C., Hebner, R., Seri, P., *et al.*: 'Partial discharge inception voltage and magnitude in polymeric cables under AC and DC voltage supply'. Jicable, Versailles, France, July 2019, pp. 1–4
[36] Seri, P., Cirioni, L., Naderiallaf, H., *et al.*: 'Partial discharge inception voltage in DC insulation systems: a comparison with AC voltage supply'. IEEE Electrical Insulation Conf., Calgary, Canada, June 2019, pp. 1–4
[37] Montanari, G. C., Seri, P., Ghosh, R., *et al.*: 'Noise rejection and partial discharge source identification in insulation system under DC voltage supply', *IEEE Trans. Dielectr. Electr. Insul.*, 2020, **27**, (2), pp. 1–6
[38] Montanari, G.C., Hebner, R.: 'Partial discharges under DC: do they exist and shall we be scared?'. IEEE PES ICC, Orlando, FL, USA, October 2018, pp. 1–9
[39] Morshuis, P.H.F., Smit, J.J.: 'Partial discharges at DC voltage: their mechanism, detection and analysis', *IEEE Trans. Dielectr. Electr. Insul.*, 2005, **12**, (2), pp. 328–340
[40] Seri, P., Naderiallaf, H., Montanari, G.C.: 'Modelling of supply voltage frequency effect on partial discharge repetition rate and charge amplitude from AC to DC. Part 1: room temperature', *IEEE Trans. Diel. El. Insulation*, 2020, **27**, pp. 1–9
[41] Occhini, E., Maschio, G.: 'Electrical characteristics of oil-impregnated paper as insulation for HV DC cables', *IEEE Trans. Power Appl. Sys.*, 1967, **86**, (3), pp. 312–326
[42] Seri, P., Ghosh, R., Naderiallaf, H., *et al.*: 'Partial discharge measurements of DC insulation systems: the influence of the energization transient'. IEEE Conf. Electrical Insulation Dielectric Phenomena, Richland, Washington, USA, October 2019, pp. 1–4
[43] Cavallini, A., Conti, M., Contin, A., *et al.*: 'Advanced PD inference in on-field measurements. Part 2: Identification of Defects in Solid Insulation', *IEEE Trans. Dielectr. and Electr. Insul.*, 2003, **10**, (3), pp. 528–538
[44] Ghosh, R., Seri, P., Montanari, G.C.: 'Condition assessment of electrical equipment in harsh electrical environment'. IEEE 4th Int. Conf. on Condition Assessment Techniques (CATCON), Chennai, India, November 2019, pp. 1–6
[45] Montanari, G.C., Palmieri, F., Mazzanti, G., *et al.*: 'AC charge injection investigated by means of space charge measurements: threshold and frequency dependence'. IEEE Int. Conf. Properties Applications Dielectric Materials, Nagoya, Japan, June 2003, pp. 895–899
[46] Wright, G.T.: 'Space-charge limited currents in insulating materials', *Nature*, 1958, **182**, pp. 1296–1297
[47] Maeno, T., Fukunaga, K.: 'High-resolution PEA charge distribution measurement system', *IEEE Trans. Dielectr. Electr. Insul.*, 1996, **3**, (6), pp. 754–757